Dalton Transactions

ROYAL SOCIETY OF CHEMISTRY

PAPER

View Article Online
View Journal | View Issue

Check for updates

Cite this: *Dalton Trans.*, 2020, **49**, 9094

Cation effects on dynamics of ligand-benzylated formazanate boron and aluminium complexes†

Ranajit Mondol and Edwin Otten *

Received 28th May 2020,
Accepted 11th June 2020

DOI: 10.1039/d0dt01918f

rsc.li/dalton

The dynamic processes present in ligand-benzylated formazanate boron and aluminium complexes are investigated using variable temperature NMR experiments and lineshape analyses. The observed difference in activation parameters for complexes containing either organic countercations (NBu_4^+) or alkali cations is rationalized on the basis of a different degree of ion-pairing in the ground state, and the data are in all cases consistent with a mechanism that involves pyramidal inversion at the nitrogens in the heterocyclic ring rather than homolytic N–C(benzyl) bond cleavage.

Introduction

Alkali cations have important roles in a biological context[1–3] and synthetic chemistry.[4–6] The noncovalent interactions of organic moieties with alkali–metal cations can have a pronounced effect on the (electronic) structure and reactivity of complexes, as exemplified by features such as geometry,[7,8] redox potentials,[9] N_2 cleavage,[10] reaction rates,[11–14] and even selectivity of chemical transformations.[15–17] Of particular relevance to the work described here is a series of reduced iron complexes with a redox-active formazanate ligand that are paired with alkali–metal countercations as reported by Broere, Holland and co-workers.[18] In the presence of a crown ether to sequester the alkali cation, the reduced iron complex was obtained as a monomer, whereas in absence of a crown ether the reduced iron complex was isolated in dimeric form (Chart 1, **A**).[18] It was demonstrated that in these dimeric compounds, the binding mode of counter cations to the ligand is dependent on the nature of the alkali–metal (Chart 1), and that this has a pronounced effect on the structure and dynamics of these compounds.[18]

The formazanate ligands used in this study have received increasing attention in the last decade following a report by Hicks and coworkers that described ligand-centered redox-reactions in a formazanate boron compound.[19] In 2014, our group has started to investigate the coordination chemistry, ligand-centered reductions and reactivity of compounds with formazanate ligands.[20–27] Concurrent with our work, the Gilroy group[28–37] and others[38–40] have synthesized a variety of compounds with formazanate ligands, and studied their optical and electrochemical properties.[41] Previously, we described that main group (B and Al) complexes with these ligands can accept up to two electrons, and that these reduction products subsequently react with electrophiles (*e.g.*, Bn^+ or H^+) to form new N–C and N–H bonds at the formazanate ligand (Scheme 1).[42–45] Furthermore, we have demonstrated that the [$2e^-/E^+$]-equivalent 'stored' at the ligand could be converted to $E^\bullet$ radicals *via* homolytic cleavage of the N–C (Bn) and N–H bonds, respectively.[43] In a recent paper, the structural features and homolytic bond dissociation energies of ligand-benzylated B and Al complexes were reported.[45] These studies suggested that the increased ionic character in the Al analogues leads to more facile bond homolysis, while the rate of benzyl transfer to TEMPO is independent on the nature of the countercation.

Here, we report a study on the dynamics of anionic, ligand-benzylated B and Al complexes by NMR lineshape analysis for the resonances of the (diastereotopic) *N*-benzyl group. Analysis of the empirical exchange rates for a series of compounds with different countercations suggests that the dynamic features are due to inversion at the nitrogen atom rather than homolytic N–C bond cleavage, and that the rate-determining step involves the formation of a separated ion-pair. The results presented

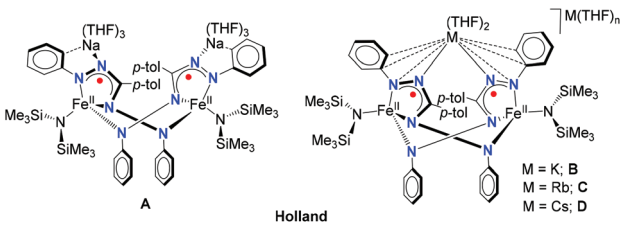

Chart 1

Stratingh Institute for Chemistry, University of Groningen, Nijenborgh 4, 9747 AG Groningen, The Netherlands. E-mail: edwin.otten@rug.nl

†Electronic supplementary information (ESI) available. See DOI: 10.1039/d0dt01918f

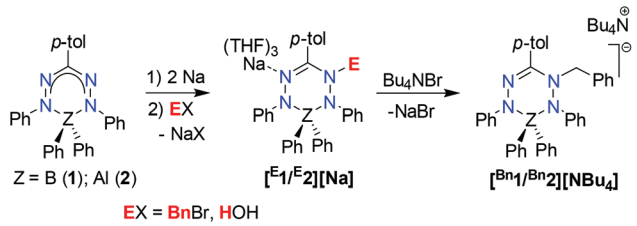

Scheme 1 Ligand-based storage of [2e$^-$/E$^+$]-equivalent in B and Al complexes with formazanate ligands.

herein emphasize the importance of coulombic and/or cation-π interactions in modulating structure and reactivity.

Results and discussion

Treatment of the two-electron reduced formazanate boron diphenyl compound $\mathbf{1}^{2-}$ with benzyl bromide afforded the ligand-benzylated anionic complex **[^{Bn}1][Na]** (Scheme 1) as reported previously.[43] The ^{1}H NMR spectrum recorded in THF-d_8 solution at room temperature showed broadened resonances for the protons at the benzylic position, which upon cooling to −5 °C became a sharp set of mutually coupled signals (δ 3.79 and 3.38 ppm; $^2J_{HH}$ = 15.3 Hz) due to the diastereotopic benzyl-CH_2 group. Conversely, measurement of the NMR spectrum at 65 °C or above showed that these resonances coalesce to a singlet (δ 3.69 ppm), indicating a dynamic process that exchanges the two diastereotopic sites. Similar dynamic features are also observed for the BPh_2 groups. In order to probe the nature of these dynamics, ^{1}H NMR spectra were collected in the temperature range between −5 and +75 °C (Fig. 1) and lineshape analysis was performed to obtain exchange rate constants. The rate of chemical exchange for the benzylic protons is found to be identical to that of the BPh_2 groups across the entire temperature range, indicating that a single dynamic process is involved. Eyring analysis afforded activation parameters for the exchange in **[^{Bn}1][Na]** as $\Delta H^{\ddagger}$ = 80.4 ± 1.7 kJ mol^{-1} and $\Delta S^{\ddagger}$ = 59.3 ± 5.6 J mol^{-1} K^{-1} (Fig. 2 and Table 1; see ESI† for details).

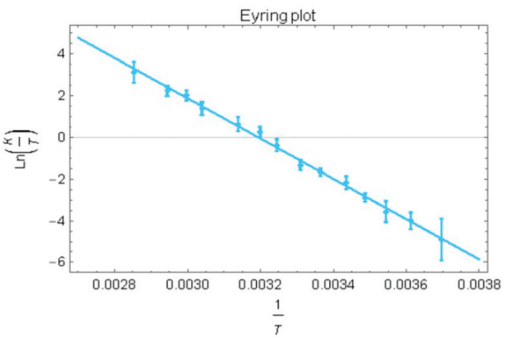

Fig. 2 Eyring plot for the determination of activation parameters for benzyl-CH_2 exchange in **[^{Bn}1][Na]**.

Table 1 Activation parameters for exchange between diastereotopic benzyl-CH_2 resonances as determined by NMR lineshape analysis

	$\Delta H^{\ddagger}$ (kJ mol^{-1})	$\Delta S^{\ddagger}$ (J mol^{-1} K^{-1})	$\Delta G^{\ddagger}_{298K}$ (kJ mol^{-1})
[^{Bn}1]$^-$			
NBu_4^+	66.7 ± 1.6	−4.2 ± 5.0	68.0
Na^+	80.4 ± 1.7	59.3 ± 5.6	62.7
K^+	68.4 ± 2.3	59.3 ± 7.3	50.7
Rb^+	72.7 ± 5.5	42.3 ± 18.0	60.1
[^{Bn}2]$^-$			
NBu_4^+	68.4 ± 1.3	−19.7 ± 3.9	74.3
Na^+	88.9 ± 2.5	56.5 ± 7.3	72.1

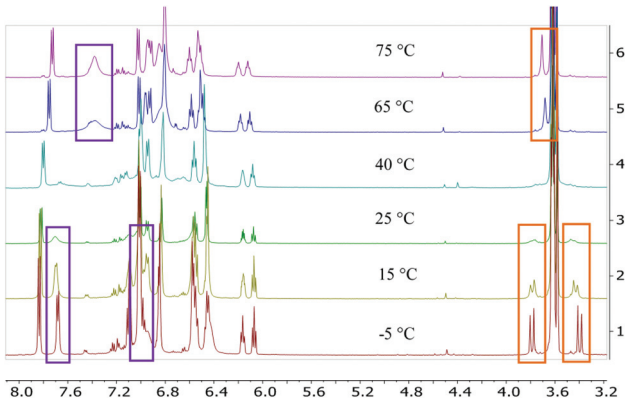

Fig. 1 Selected variable temperature ^{1}H NMR spectra of **[^{Bn}1][Na]** in THF-d_8. The resonances indicated in the orange boxes (δ 3.4–3.8 ppm) are for the benzyl-CH_2 group, those in the aromatic range (δ 7.0–7.8 ppm, purple box) are for the BPh_2 groups.

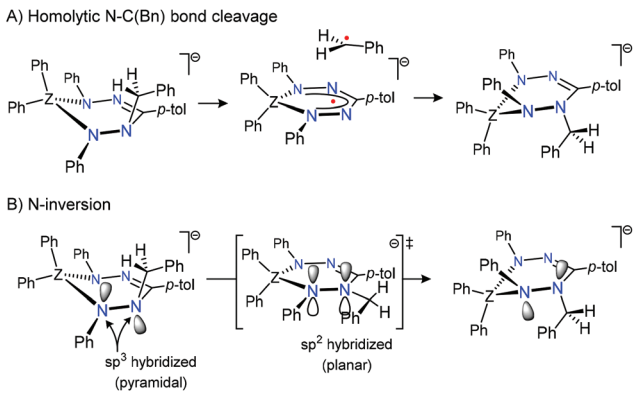

Scheme 2 Schematic representation of possible mechanisms to account for exchange between the diastereotopic benzyl CH_2 resonances in anions [^{Bn}1/2]$^-$.

The large, positive entropy of activation suggests a substantial degree of bond-breaking in the rate-determining step. Although homolytic N–C(benzyl) bond cleavage to generate Bn$^{\bullet}$ and $\mathbf{1}^{\bullet-}$ (Scheme 2A) is a potential mechanism for exchange of the diastereotopic environments in **[^{Bn}1][Na]** and is consistent with the empirical value for $\Delta S^{\ddagger}$, our previous data for the N–C(benzyl) bond dissociation energy in **[^{Bn}1][Na]** (BDE = 121 ± 5 kJ mol^{-1}; measured *via* Bn$^{\bullet}$ transfer to

TEMPO)[43] is significantly higher than the activation enthalpy for exchange ($\Delta H^{\ddagger}$ = 80.4 (1.7) kJ mol^{-1}). This rules out that bond homolysis is operative as a mechanism for site exchange in [^{Bn}**1**][**Na**].

Alternatively, the observed dynamics in [^{Bn}**1**][**Na**] could be due to pyramidal inversion *via* a planar transition state with sp^2-hybridized, trigonal planar geometries around the hydrazine nitrogen atoms (Scheme 2B). Pyramidal nitrogen inversion is a facile, low-barrier process in the majority of N-containing compounds, but substantial activation energies have been reported when the N-atom is part of a (hetero)cyclic ring.[46–50] However, nitrogen inversion is an intra-molecular process that would be expected to have an activation entropy close to zero, or (in the case of highly strained systems) a slightly negative value.[46–48]

Although both homolytic N–C bond cleavage and N-inversion are plausible mechanisms to explain the dynamics observed for [^{Bn}**1**][**Na**], neither of the two can be reconciled with the activation parameters determined experimentally. It thus appears that the rate-determining step as probed by the NMR lineshape analysis may *precede* the actual exchange of the diastereotopic sites. To investigate whether (partial) dissociation of the Na$^+$ cation in [^{Bn}**1**][**Na**] could play a role, we subsequently examined the exchange rate in the corresponding tetrabutylammonium salt [^{Bn}**1**][**NBu$_4$**].[45] In this compound, the organic cation Bu$_4$N$^+$ does not interact with the [^{Bn}**1**]$^-$ moiety other than through electrostatic interactions (*i.e.*, it forms a solvent-separated ion pair in solution; Scheme 1).[45] While the low-temperature ^{1}H NMR spectra for both compounds are very similar, the extent of line-broadening for the diastereotopic benzyl-CH$_2$ group at a given temperature is quite different between the two, which indicates that these compounds have distinct exchange rates. Lineshape analysis on NMR spectral data collected between 25 and 85 °C allowed the activation parameters for the exchange process in [^{Bn}**1**][**NBu$_4$**] to be determined as $\Delta H^{\ddagger}$ = 66.7 ± 1.6 kJ mol^{-1} and $\Delta S^{\ddagger}$ = −4.2 ± 5.0 J mol^{-1} K^{-1} (Table 1; see ESI† for details). A comparison between these values to the ones measured for the sodium salt [^{Bn}**1**][**Na**] reveals striking differences, despite the fact that the anionic boron complex undergoing exchange is identical: both the entropy and enthalpy of activation are significantly lower in the tetrabutylammonium salt, with values for $\Delta S^{\ddagger}$ changing from positive (+59.3 ± 5.6 J mol^{-1} K^{-1} in [^{Bn}**1**][**Na**]) to slightly negative (−4.2 ± 5.0 J mol^{-1} K^{-1} for [^{Bn}**1**][**NBu$_4$**]). The latter value is fully consistent with an intramolecular nitrogen inversion process.[46–48] Thus, we conclude that in the absence of a coordinating countercation in [^{Bn}**1**][**NBu$_4$**], the activation parameters reflect the intrinsic values for the exchange process, *i.e.* pyramidal N-inversion, whereas in [^{Bn}**1**][**Na**] this step is obscured by the involvement of cation–anion dissociation as part of the rate-determining step.

Although the overall barrier to nitrogen inversion ($\Delta G^{\ddagger}$ (298 K) = 68.0 kJ mol^{-1} for [^{Bn}**1**][**NBu$_4$**]) is higher than that in simple amines (21–42 kJ mol^{-1}),[51–53] or in bicyclic hydrazines (*e.g.*, 49.4 kJ mol^{-1} in 2,3-dimethyl-2,3-diazabicyclo[2.2.2]octane),[54] it should be noted that in the six-membered boron heterocycle [^{Bn}**1**]$^-$ the N-inversion occurs concurrent with exchange of the BPh$_2$ environments, indicating a correlated ('geared') movement of the entire heterocycle (and its substituents). In support of this interpretation we note that Neugebauer and Mannschreck reported slow N-inversion in related all-organic, neutral 1,2,3,4-tetrahydro-*s*-tetrazines (leucoverdazyls), which were found to have activation free energies between *ca.* 52 and 83 kJ mol^{-1} based on determination of coalescence temperatures.[55] Our previously published X-ray crystal structure for [^{Bn}**1**][**NBu$_4$**][45] provides additional insight in the origin of the high barrier: simultaneous inversion of both hydrazine-type nitrogens (the adjacent N–Ph and N–Bn atoms) *via* a planar transition state likely causes substantial steric hindrance in this densely substituted heterocycle.

To further corroborate the importance of ion-pair dissociation in these systems, we investigated complexes with heavier alkali cations. Synthesis of salts of [^{Bn}**1**]$^-$ with K$^+$ and Rb$^+$ counterions was achieved by treatment of **1** with 2 equiv. of KC$_8$ or RbC$_8$, followed by addition of benzyl bromide. Similar to [^{Bn}**1**][**Na**],[43] the UV/Vis spectra of the isolated ligand-benzylated compounds [^{Bn}**1**][**K**] and [^{Bn}**1**][**Rb**] have absorption maxima at 396 nm (Fig. S1†), and the ^{1}H NMR spectra show diastereotopic signals for the benzyl-CH$_2$ group and line-broadening indicative of exchange (see ESI† for details). Overall, the ^{1}H NMR spectra in this series are comparable,[45] although there are noticeable differences in chemical shifts (in particular for the Rb$^+$-salt) that suggest that the heavier alkali metals interact differently with the anion [^{Bn}**1**]$^-$. A similar trend was observed in anionic formazanate iron complexes,[18] and a possible explanation may be the different stability for π- *vs.* σ-bonding between the alkali metal cation and these anionic heterocycles.

The aluminum analogue [^{Bn}**2**]$^-$ was investigated to probe the effect of the central group 13 element on the observed dynamics. Both the sodium salt [^{Bn}**2**][**Na**] and the tetrabutylammonium analogue [^{Bn}**2**][**NBu$_4$**] were synthesized according to the published procedures,[45] and a variable NMR spectroscopic study reveals that chemical exchange also occurs in these compounds (Fig. S14 and S13†). Lineshape analysis afforded activation parameters for [^{Bn}**2**][**Na**] as $\Delta H^{\ddagger}$ = 88.9 (2.5) kJ mol^{-1} and $\Delta S^{\ddagger}$ = 56.5 ± 7.3 J mol^{-1} K^{-1}, whereas the corresponding values for [^{Bn}**2**][**NBu$_4$**] are $\Delta H^{\ddagger}$ = 68.4 ± 1.3 kJ mol^{-1} and $\Delta S^{\ddagger}$ = −19.7 ± 3.9 J mol^{-1} K^{-1} (Table 1; see ESI† for details). Thus, the change in countercation from Na$^+$ to Bu$_4$N$^+$ results again in markedly different activation entropies for these two compounds: $\Delta S^{\ddagger}$ is large/positive when the cation (Na$^+$) is bound to the ligand backbone, whereas it is negative when this is not the case (Table 1). As in the boron analogues [^{Bn}**1**]$^-$, we interpret this as a changeover in the rate-determining step from a genuine N-inversion step to dissociation of the coordinating cation. Comparison of the Bu$_4$N$^+$ salts of the boron and aluminum complexes shows similar values for $\Delta H^{\ddagger}$, indicating that the intrinsic effect of the central element on nitrogen inversion is small. The increase in $\Delta H^{\ddagger}$ for the

sodium salt of the Al heterocycle [^{Bn}**2**][**Na**] compared to the boron analogue ([^{Bn}**2**][**Na**]) is consistent with our previous results that bonding in the Al complex is significantly more ionic in nature: the benzylated formazanate ligand in [^{Bn}**2**]$^-$ bears more negative charge,[45] and thus has stronger electrostatic interactions with the Na^+ cation.

Conclusions

The NMR study presented here shows that the dynamics in ligand-benzylated formazanate boron and aluminium compounds (*i.e.*, ^{Bn}**1**$^-$ and ^{Bn}**2**$^-$) is due to nitrogen inversion rather than homolytic N–C bond cleavage. The observation that the activation parameters for exchange in these anions are highly dependent on the nature of the countercation highlights the importance of alkali cation in modulating rates of reactions as simple as nitrogen inversion. Specifically, we conclude that the divergent activation parameters of salts of [^{Bn}**1**/**2**]$^-$ with either alkali or organic cations is due to a difference in ion-pairing in the ground state. When there is no specific interaction between the anionic group 13 complex and the cation (*i.e.*, in the solvent-separated ion pairs with NBu_4^+), the activation parameters reflect the intrinsic barrier for nitrogen inversion, whereas for the compounds with alkali cations there is a significant contribution from dissociation of the ion pair.

Conflicts of interest

There are no conflicts to declare.

Acknowledgements

Financial support from the Netherlands Organisation for Scientific Research (NWO) (VIDI grant to EO) is gratefully acknowledged.

Notes and references

1 *The Alkali Metal Ions: Their Role for Life*, ed. A. Sigel, H. Sigel and R. K. O. Sigel, Springer International Publishing, Cham, 2016, vol. 16.
2 D. A. Dougherty, *Science*, 1996, **271**, 163–168.
3 J. C. Ma and D. A. Dougherty, *Chem. Rev.*, 1997, **97**, 1303–1324.
4 R. Oukaci, J. C. S. Wu and J. G. Goodwin, *J. Catal.*, 1987, **107**, 471–481.
5 F. J. Williams, A. Palermo, M. S. Tikhov and R. M. Lambert, *Surf. Sci.*, 2001, **482–485**, 177–182.
6 G. P. Connor and P. L. Holland, *Catal. Today*, 2017, **286**, 21–40.
7 S. F. McWilliams, K. R. Rodgers, G. Lukat-Rodgers, B. Q. Mercado, K. Grubel and P. L. Holland, *Inorg. Chem.*, 2016, **55**, 2960–2968.
8 G. González-Riopedre, M. R. Bermejo, M. I. Fernández-García, A. M. González-Noya, R. Pedrido, M. J. Rodríguez-Doutón and M. Maneiro, *Inorg. Chem.*, 2015, **54**, 2512–2521.
9 A. H. Reath, J. W. Ziller, C. Tsay, A. J. Ryan and J. Y. Yang, *Inorg. Chem.*, 2017, **56**, 3713–3718.
10 K. Grubel, W. W. Brennessel, B. Q. Mercado and P. L. Holland, *J. Am. Chem. Soc.*, 2014, **136**, 16807–16816.
11 M. R. Kita and A. J. M. Miller, *Angew. Chem., Int. Ed*, 2017, 56, 5498–5502.
12 M. R. Kita and A. J. M. Miller, *J. Am. Chem. Soc.*, 2014, **136**, 14519–14529.
13 C. M. Moore, B. Bark and N. K. Szymczak, *ACS Catal.*, 2016, **6**, 1981–1990.
14 H. Bosch, J. G. Van Ommen and P. J. Gellings, *Appl. Catal.*, 1985, **18**, 405–408.
15 R. Y. Rohling, E. J. M. Hensen and E. A. Pidko, *ChemPhysChem*, 2018, **19**, 446–458.
16 J. Sivaguru, A. Natarajan, L. S. Kaanumalle, J. Shailaja, S. Uppili, A. Joy and V. Ramamurthy, *Acc. Chem. Res.*, 2003, **36**, 509–521.
17 L. M. Jackman and B. C. Lange, *Tetrahedron*, 1977, **33**, 2737–2769.
18 D. L. J. Broere, B. Q. Mercado, E. Bill, K. M. Lancaster, S. Sproules and P. L. Holland, *Inorg. Chem.*, 2018, **57**, 9580–9591.
19 J. B. Gilroy, M. J. Ferguson, R. McDonald, B. O. Patrick and R. G. Hicks, *Chem. Commun.*, 2007, 126–128.
20 M. C. Chang, T. Dann, D. P. Day, M. Lutz, G. G. Wildgoose and E. Otten, *Angew. Chem., Int. Ed.*, 2014, **53**, 4118–4122.
21 M.-C. Chang and E. Otten, *Chem. Commun.*, 2014, **50**, 7431–7433.
22 R. Travieso-Puente, M. C. Chang and E. Otten, *Dalton Trans.*, 2014, **43**, 18035–18041.
23 R. Travieso-Puente, J. O. P. Broekman, M. C. Chang, S. Demeshko, F. Meyer and E. Otten, *J. Am. Chem. Soc.*, 2016, **138**, 5503–5506.
24 M. C. Chang and E. Otten, *Organometallics*, 2016, **35**, 534–542.
25 M. C. Chang, A. Chantzis, D. Jacquemin and E. Otten, *Dalton Trans.*, 2016, **45**, 9477–9484.
26 M. C. Chang, P. Roewen, R. Travieso-Puente, M. Lutz and E. Otten, *Inorg. Chem.*, 2015, **54**, 379–388.
27 M.-C. Chang and E. Otten, *Inorg. Chem.*, 2015, **54**, 8656–8664.
28 S. M. Barbon, J. T. Price, P. A. Reinkeluers and J. B. Gilroy, *Inorg. Chem.*, 2014, **53**, 10585–10593.
29 M. Hesari, S. M. Barbon, V. N. Staroverov, Z. Ding and J. B. Gilroy, *Chem. Commun.*, 2015, **51**, 3766–3769.
30 S. M. Barbon, J. T. Price, U. Yogarajah and J. B. Gilroy, *RSC Adv.*, 2015, **5**, 56316–56324.
31 S. M. Barbon, J. V. Buddingh, R. R. Maar and J. B. Gilroy, *Inorg. Chem.*, 2017, **56**, 12003–12011.
32 S. Novoa and J. B. Gilroy, *Polym. Chem.*, 2017, **8**, 5388–5395.
33 S. M. Barbon, S. Novoa, D. Bender, H. Groom, L. G. Luyt and J. B. Gilroy, *Org. Chem. Front.*, 2017, **4**, 178–190.

34 S. M. Barbon, V. N. Staroverov and J. B. Gilroy, *Angew. Chem., Int. Ed.*, 2017, **129**, 8285–8289.
35 R. R. Maar, A. Rabiee Kenaree, R. Zhang, Y. Tao, B. D. Katzman, V. N. Staroverov, Z. Ding and J. B. Gilroy, *Inorg. Chem.*, 2017, **56**, 12436–12447.
36 J. S. Dhindsa, R. R. Maar, S. M. Barbon, M. Olivia Avilés, Z. K. Powell, F. Lagugné-Labarthet and J. B. Gilroy, *Chem. Commun.*, 2018, **54**, 6899–6902.
37 A. Van Belois, R. R. Maar, M. S. Workentin and J. B. Gilroy, *Inorg. Chem.*, 2019, **58**, 834–843.
38 A. Mandal, B. Schwederski, J. Fiedler, W. Kaim and G. K. Lahiri, *Inorg. Chem.*, 2015, **54**, 8126–8135.
39 G. Mu, L. Cong, Z. Wen, J. I. C. Wu, K. M. Kadish and T. S. Teets, *Inorg. Chem.*, 2018, **57**, 9468–9477.
40 E. Kabir, D. Patel, K. Clark and T. S. Teets, *Inorg. Chem.*, 2018, **57**, 10906–10917.
41 J. B. Gilroy and E. Otten, *Chem. Soc. Rev.*, 2020, **49**, 85–113.
42 R. Mondol, D. A. Snoeken, M.-C. Chang and E. Otten, *Chem. Commun.*, 2017, **53**, 513–516.
43 R. Mondol and E. Otten, *Inorg. Chem.*, 2018, **57**, 9720–9727.
44 R. Mondol and E. Otten, *Inorg. Chem.*, 2019, **58**, 6344–6355.
45 R. Mondol and E. Otten, *Dalton Trans.*, 2019, **48**, 13981–13988.
46 F. A. L. Anet, R. D. Trepka and D. J. Cram, *J. Am. Chem. Soc.*, 1967, **89**, 357–362.
47 J. H. Hall and W. S. Bigard, *J. Org. Chem.*, 1978, **43**, 2785–2788.
48 J. E. Anderson and J. M. Lehn, *J. Am. Chem. Soc.*, 1967, **89**, 81–87.
49 A. Rauk, L. C. Allen and K. Mislow, *Angew. Chem., Int. Ed. Engl.*, 1970, **9**, 400–414.
50 (*a*) A. R. Katritzky, R. C. Patel and F. G. Riddell, *J. Chem. Soc., Chem. Commun.*, 1979, 674; (*b*) A. R. Katritzky, R. C. Patel and F. G. Riddell, *Angew. Chem., Int. Ed.*, 1981, 521–529.
51 A. Rauk, L. C. Allen and K. Mislow, *Angew. Chem., Int. Ed. Engl.*, 1970, **9**, 400–414.
52 J. B. Lambert and W. L. Oliver, *J. Am. Chem. Soc.*, 1969, **91**, 7774–7775.
53 C. D. Montgomery, *J. Chem. Educ.*, 2013, **90**, 661–664.
54 J. E. Anderson and J. M. Lehn, *J. Am. Chem. Soc.*, 1967, **89**, 81–87.
55 F. A. Neugebauer and A. Mannschreck, *Tetrahedron*, 1972, **28**, 2533–2538.